

Probing anomalous tbW couplings in single-top production using top polarization at the Large Hadron Collider

Saurabh D. Rindani* and Pankaj Sharma†

*Theoretical Physics Division, Physical Research Laboratory,
Navrangpura, Ahmedabad 380 009, India*

Abstract

We study the sensitivity of the Large Hadron Collider (LHC) to anomalous tbW couplings in single-top production in association with a W^- boson followed by semileptonic decay of the top. We calculate top polarization and the effects of these anomalous couplings to it at two centre-of-mass (cm) energies of 7 TeV and 14 TeV. As a measure of top polarization, we look at various laboratory frame distributions of its decay products, viz., lepton angular and energy distributions and b -quark angular distributions, without requiring reconstruction of the rest frame of the top, and study the effect of anomalous couplings on these distributions. We construct certain asymmetries to study the sensitivity of these distributions to anomalous tbW couplings. We find that 1σ limits on real and imaginary parts of the dominant anomalous coupling f_{2R} which may be obtained by utilizing these asymmetries at the LHC with cm energy of 14 TeV and an integrated luminosity of 10 fb^{-1} will be significantly better than the expectations from direct measurements of cross sections and some other variables at the LHC and over an order of magnitude better than the indirect limits.

* saurabh@prl.res.in

† pankajs@prl.res.in

I. INTRODUCTION

Since the discovery of the top quark at Tevatron [1], its properties have been studied extensively, in particular its mass [2]. With a mass $m_t = 172.6 \pm 1.4$ GeV close to the electroweak (EW) scale, the top quark is widely considered to be a key to the understanding of the mechanism of electroweak symmetry breaking. Owing to its large mass, its decay width $\Gamma_t = 1.3$ GeV is very small, leading to an extremely short life time, $\tau_t = 1/\Gamma_t \simeq 5 \times 10^{-25}$ s. This is an order of magnitude smaller than the hadronization time scale $\tau_{had} \simeq 1/\Lambda_{QCD} \sim 3 \times 10^{-24}$ s, and hence it decays before any non-perturbative effects can spoil its spin information. As a consequence, its polarization can be determined through the angular and/or energy distributions of its decay products [3]. The degree of polarization of the top quark may be a probe of any new physics responsible for its production. Top-quark polarization has been suggested for the study of new physics models in top-pair as well as single-top production at hadron colliders [4–8].

At the Large Hadron Collider (LHC), top quarks will be produced mainly in pairs dominantly through gluon fusion whose contribution to the cross section is 90%, while quark-antiquark annihilation contributes 10%. Both these production mechanisms proceed mainly through QCD interactions. Since gluon couplings are chirality-conserving, the polarization of top quarks can arise only through the Z -exchange contribution to $q\bar{q}$ annihilation channel, and is expected to be very small. However, single-top production can also occur [9–16, 19, 21], and has already been seen [22]. Since it proceeds via weak interactions, top quarks will have large polarization [15, 16]. At LHC energies, single-top quark events in the SM are expected to be produced via a) the t -channel ($bq \rightarrow tq'$) process, b) the s -channel process ($q\bar{q}' \rightarrow t\bar{b}$) and c) the tW associated production process ($bg \rightarrow tW^-$) [13]. In all these processes, there is at least one chiral vertex which gives rise to large top polarization. The three processes are completely different kinematically and can be separated from each other. In this work, we study in detail the effect of anomalous tbW vertex on top polarization in associated production of the top quark with a W boson.

Among all top couplings to gauge and Higgs bosons, the tbW vertex deserves special attention since the top quark is expected to decay almost completely via this interaction. However, in several extensions of SM, as for example supersymmetry and models of dynamical symmetry breaking, sizable deviations are possible from the SM predictions and also new decays of top quarks are possible. These deviations of the tbW vertex may be observed in top decays. Single-top production is another source to study deviation in the tbW vertex. For on-shell top, bottom and W , the most general effective vertices for the tbW interaction up to dimension five can be written as [23]

$$V_{t \rightarrow bW^+} = \frac{-g}{\sqrt{2}} V_{tb} \left[\gamma^\mu (f_{1L} P_L + f_{1R} P_R) - \frac{i\sigma^{\mu\nu}}{m_W} (p_t - p_b)_\nu (f_{2L} P_L + f_{2R} P_R) \right] \quad (1)$$

for the decay $t \rightarrow bW^+$, and

$$V_{b \rightarrow tW^-} = \frac{-g}{\sqrt{2}} V_{tb}^* \left[\gamma^\mu (f_{1L}^* P_L + f_{1R}^* P_R) - \frac{i\sigma^{\mu\nu}}{m_W} (p_t - p_b)_\nu (f_{2R}^* P_L + f_{2L}^* P_R) \right] \quad (2)$$

for tW^- production from a virtual b , where V_{tb} is the Cabibbo-Kobayashi-Maskawa matrix element, and f_{1L} , f_{2L} , f_{1R} , f_{2R} are couplings. In the SM, $f_{1L} = 1$ and $f_{1R} = f_{2L} = f_{2R} = 0$. We have assumed all the anomalous couplings to be complex and treat real and imaginary

parts of these couplings as independent parameters. We assume CP to be conserved in this analysis. Various extensions of the SM would have specific predictions for these anomalous couplings. For example, the contributions to these form factors in two Higgs doublet model (2HDM), minimal supersymmetric standard model (MSSM) and top-color assisted Technicolor model (TC2) have been evaluated in Ref. [24].

Tevatron provides the only existing direct limits on anomalous tbW couplings through W polarization measurements. Recently, CDF II with 2.7 fb^{-1} of collected data reported results for the longitudinal and right-handed helicity fractions of the W boson in semileptonic top-decays [17]. D0 also reported results on W helicity fractions using a combination of semileptonic and dilepton decay channels [18]. These results on W polarization measurements led to a limit of $[-0.3, 0.3]$ on f_{2R} at the 95% confidence level (CL) [19] in single-top production. The CMS and ATLAS collaborations have also reported the W helicity fractions with early LHC data [20]. In Ref. [21], the authors have used the recent top quark decay asymmetries from ATLAS and the t -channel single-top cross section from CMS to put the limits on tbW couplings. They find that despite the small statistics available, the early LHC limits of $[-0.6, 0.3]$ on f_{2R} are not too far from the Tevatron limits.

Apart from direct measurements at the LHC and Tevatron, there are stringent indirect constraints coming from low-energy measurements of anomalous tbW couplings. The measured rate of $b \rightarrow s\gamma$ puts stringent constraints on the couplings f_{1R} and f_{2L} of about 4×10^{-3} , since their contributions to B -meson decay get an enhancement factor of m_t/m_b [25–28]. The bound on the anomalous coupling f_{2R} is very weak, $[-0.15, 0.57]$ at 95 % CL. These bounds are obtained by taking one coupling to be non-zero at a time. However if one allows all couplings to be non-zero simultaneously, there is a possibility of cancellations among contributions of different couplings and the limits on these couplings could be very different.

Single-top production in association with a W^- boson can be used to probe the size and nature of the tbW couplings. Apart from the cross section, the angular distribution of the top, and even the polarization of the top would give additional information enabling the determination of the tbW coupling. Here we focus on the polarization of the top produced in the tW associated production process. The most direct way to determine top polarization is by measuring the angular distribution of its decay products in its rest frame. However, at the LHC reconstructing the top rest frame is difficult and will result in large systematic uncertainties. In this paper, we show how the decay lepton angular distributions in the laboratory (lab) frame can be a useful probe of top polarization and hence of anomalous tbW^- couplings.

In this context it is interesting to recall that the angular distribution of the charged lepton is independent of anomalous tbW couplings in the decay of the top quark, to linear order in the anomalous couplings (the “decoupling theorem”) [29, 30]. Hence, the lepton angular distribution may be considered to be a pure and robust probe of any new physics involved in the production of the top quark. In this analysis, we study the angular distribution of the charged lepton without making the approximation that anomalous couplings are small and include higher-order terms in anomalous couplings. We also study the distributions to linear order in the anomalous couplings in the region of validity of the decoupling theorem. In this way, we investigate the range of anomalous couplings for which the decoupling theorem is valid. We find that the azimuthal distribution of the lepton is sensitive to top polarization and can be used to probe the form factor f_{2R} . The use of laboratory-frame charged-lepton azimuthal distribution for the measurement of top polarization in $t\bar{t}$ production at the LHC

in a certain class of Z' models was demonstrated in [6].

While charged-lepton angular distributions, at least for small values of anomalous couplings, would be a direct measure of top polarization, and hence would probe anomalous tbW couplings in tW^- production, other kinematic distributions could also be used to study anomalous tbW couplings. Thus, the charged-lepton energy distribution and the decay- b angular distribution, which do not obey the decoupling theorem, would depend on top polarization as well as anomalous couplings in top decay. Thus they would get contributions from tbW couplings in production as well as in decay. We have thus also studied the charged-lepton energy distribution and the b -quark angular distribution as probes of anomalous tbW couplings. In all cases, we obtain analytical expressions for the parton-level distributions at leading order in the couplings.

The effects of top polarization in tW and tH^- production have been studied previously in [4, 31]. Ref. [31] included the effects of one-loop EW SUSY corrections. It did not however include top decay. Top polarization in different modes of single-top production has also been studied in [14, 15], where spin-sensitive variables were used to analyze effective left- and right-handed couplings of the top coming from physics beyond the SM.

The rest of the paper is organized as follows. In the next section we discuss the cross section for single-top production in association with a W^- , the corresponding top angular distribution, as well as top polarization in the process, obtaining analytical expressions and evaluating them numerically. In Sec. III, we obtain expressions for charged-lepton angular and energy distributions, and in Sec. IV we obtain the b -quark angular distribution. In case of each distribution, we evaluate an asymmetry as a variable sensitive to tbW anomalous couplings. Sec. V contains an analysis of the sensitivities of the various asymmetries to the anomalous couplings. In Sec. VI we discuss briefly the backgrounds and non-leading corrections to our signal process, and conclude in Sec. VII. The Appendix contains certain lengthy mathematical expressions.

II. SINGLE-TOP PRODUCTION IN ASSOCIATION WITH A W BOSON

As stated earlier, single-top production at hadron colliders occurs through three different modes. All these three modes are distinct in terms of initial and final states and are in principle separately measurable. The tW^- mode of single-top production is distinct from other two modes in the sense that it is affected by the new physics only in the tbW vertex while, in other modes, there may be exotic scalars or gauge bosons which can give additional contributions to the process. The tW^- mode of single-top production has been studied in detail in Ref. [13]. At the parton level, the tW^- production proceeds through a gluon and a bottom quark each coming from a proton and gets contribution from two diagrams. Feynman diagrams for the process $g(p_g)b(p_b) \rightarrow t(p_t, \lambda_t)W^-$ are shown in Fig. 1, where $\lambda_t = \pm 1$ represent the top helicity and the blobs denote effective tbW vertices, including anomalous couplings, in the production process. These couplings are also involved in the decay of the top as shown in Fig. 2.

We obtain analytical expressions for the spin density matrix for tW production including anomalous couplings. Use was made of the analytic manipulation program FORM [32]. We find that at linear order, only the real part of the coupling f_{2R} gives significant contribution to the production density matrix, whereas contributions from all other couplings are proportional to the mass of b quark (which we neglect consistently) and hence vanish in the limit of zero bottom mass. To second order in anomalous couplings, other anomalous couplings

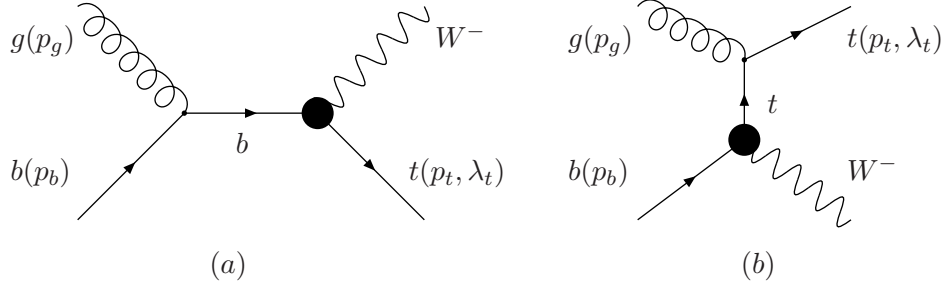


FIG. 1: Feynman diagrams contributing to associated tW^- production at the LHC.

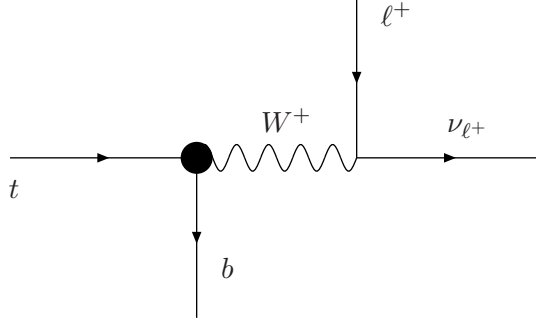


FIG. 2: Anomalous tbW couplings in top decay

do contribute, but we focus only on f_{2R} , since its contribution, arising at linear order, is dominant. Expressions for the spin density matrix elements $\rho(\pm, \pm)$ and $\rho(\pm, \mp)$ for tW production, where \pm are the signs of the top-quark helicity, are given in the Appendix.

A. Production cross section

After integrating the density matrix given in the Appendix over the phase space, the diagonal elements of this integrated density matrix, which we denote by $\sigma(+, +)$ and $\sigma(-, -)$, are respectively the cross sections for the production of positive and negative helicity tops and $\sigma_{\text{tot}} = \sigma(+, +) + \sigma(-, -)$ is the total cross section.

For numerical calculations, we use the leading-order parton distribution function (PDF) sets of CTEQ6L [33] with a factorization scale of $m_t = 172.6$ GeV. We also evaluate the strong coupling at the same scale, $\alpha_s(m_t) = 0.1085$. We make use of the following values of other parameters: $M_W = 80.403$ GeV, the electromagnetic coupling $\alpha_{em}(m_Z) = 1/128$ and $\sin^2 \theta_W = 0.23$. We set $f_{1L} = 1$ and $V_{tb} = 1$ in our calculations. We take only one coupling to be non-zero at a time in the analysis, except in Sec.V.

In Fig. 3, we show the cross section as a function of various anomalous tbW couplings for two different values of centre-of-mass (cm) energies of 7 TeV and 14 TeV for which the LHC is planned to operate. We show contributions of anomalous couplings to the cross section at linear order as well as without the approximation. From Fig. 3, one can infer that the

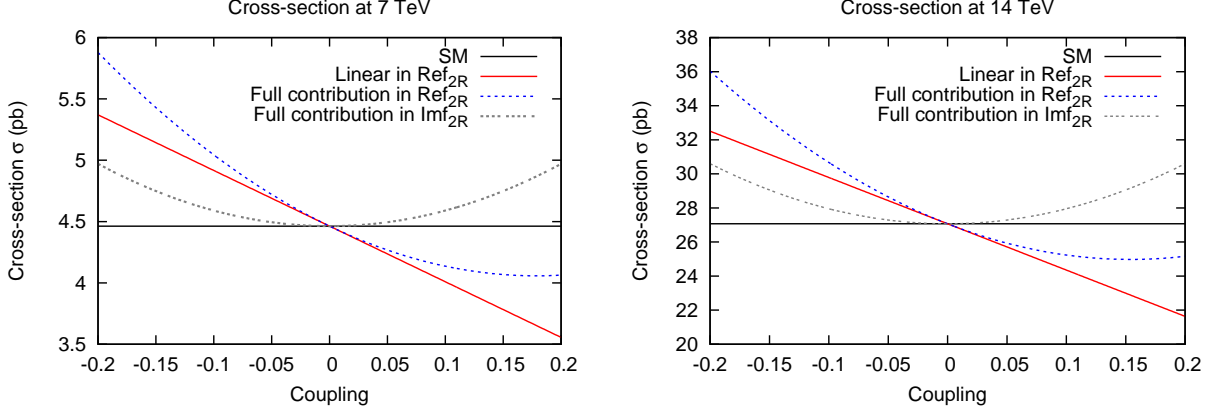


FIG. 3: The cross section for tW^- production at the LHC for two different cm energies, 7 TeV (left) and 14 TeV (right), as a function of anomalous tbW couplings.

cross section is very sensitive to negative values of Ref_{2R} . The linear approximation is seen to be good for values of anomalous coupling ranging from -0.05 to 0.05 .

Since the cross section may receive large radiative corrections at the LHC, we focus on using observables like asymmetries which are ratios of some partial cross sections, and which are expected to be insensitive to such corrections.

B. Top-angular distribution

The angular distribution of the top quark would be modified by anomalous couplings. Since the top quark is produced in a $2 \rightarrow 2$ process, its azimuthal distribution is flat. We can study its polar distribution with the polar angle defined with respect to either of the beam directions as the z axis. We find that the polar distribution is sensitive to anomalous tbW couplings. The normalized polar distribution is plotted in Fig. 4 for cm energies 7 TeV

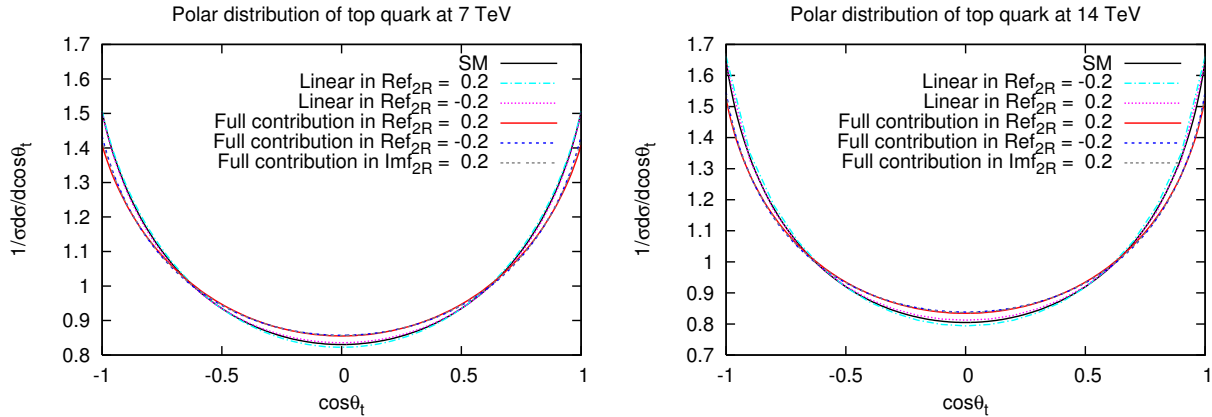


FIG. 4: The top-polar angular distributions for tW^- production at the LHC for two different cm energies, 7 TeV (left) and 14 TeV (right), for different anomalous tbW couplings.

and 14 TeV.

As can be seen from Fig. 4, the curves for the polar distributions for the SM and for the anomalous couplings of magnitude 0.2 are separated from each other. The top distribution has no forward-backward asymmetry, the colliding beams being identical. However, we can define an asymmetry utilizing the polar distributions of the top quark as

$$\mathcal{A}_\theta^t = \frac{\sigma(|z| > 0.5) - \sigma(|z| < 0.5)}{\sigma(|z| > 0.5) + \sigma(|z| < 0.5)} \quad (3)$$

where z is $\cos\theta_t$. We plot this asymmetry as a function of anomalous tbW couplings for

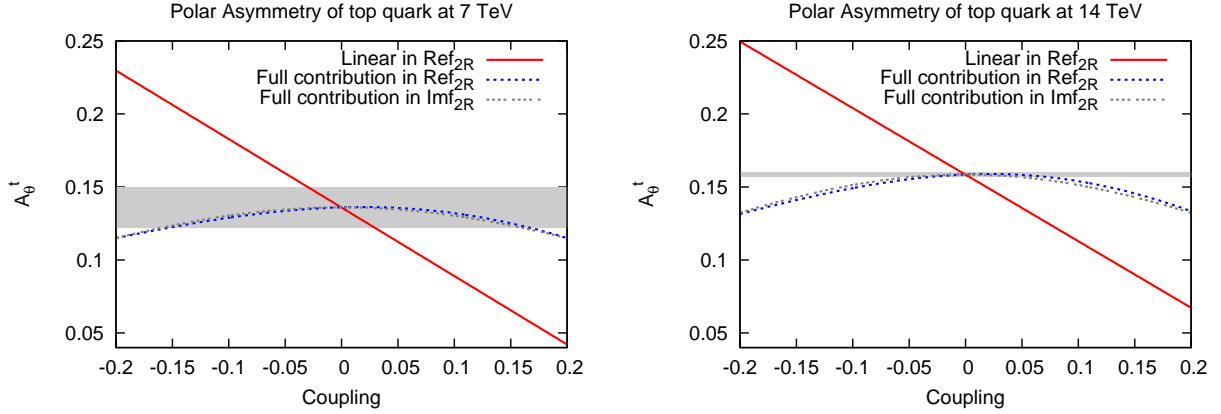


FIG. 5: The top polar asymmetries for tW^- production at the LHC for two different cm energies, 7 TeV (left) and 14 TeV (right), as a function of anomalous tbW couplings. The grey band corresponds to the top-polar asymmetry predicted in the SM with a 1σ error interval.

two cm of energies $\sqrt{s} = 7$ TeV and 14 TeV in Fig. 5. A_t^θ deviates more than 1σ from its SM value for Ref_{2R} and Imf_{2R} close to ± 0.2 for $\sqrt{s} = 7$ TeV, but is much more sensitive for $\sqrt{s} = 14$ TeV.

The asymmetry \mathcal{A}_θ^t requires accurate determination of the top direction in the lab frame and a quantitative estimate of its sensitivity to anomalous couplings needs details of the efficiency of reconstruction of the direction. We do not study this asymmetry any further, but proceed to a discussion of top polarization.

C. Top polarization

The degree of longitudinal polarization P_t of the top quark is given by

$$P_t = \frac{\sigma(+,+) - \sigma(-,-)}{\sigma(+,+) + \sigma(-,-)}. \quad (4)$$

This polarization asymmetry is shown in Fig. 6 as a function of anomalous couplings in the linear approximation, as well as without approximation, for $\sqrt{s} = 7$ TeV and 14 TeV. As compared to the SM value of -0.256 for $\sqrt{s} = 14$ TeV, the degree of longitudinal top polarization varies from -0.07 to -0.28 for Ref_{2R} varied over the range -0.2 to $+0.2$, while it varies from -0.14 to -0.25 for the same range of Imf_{2R} , and is symmetric about $\text{Imf}_{2R} = 0$.

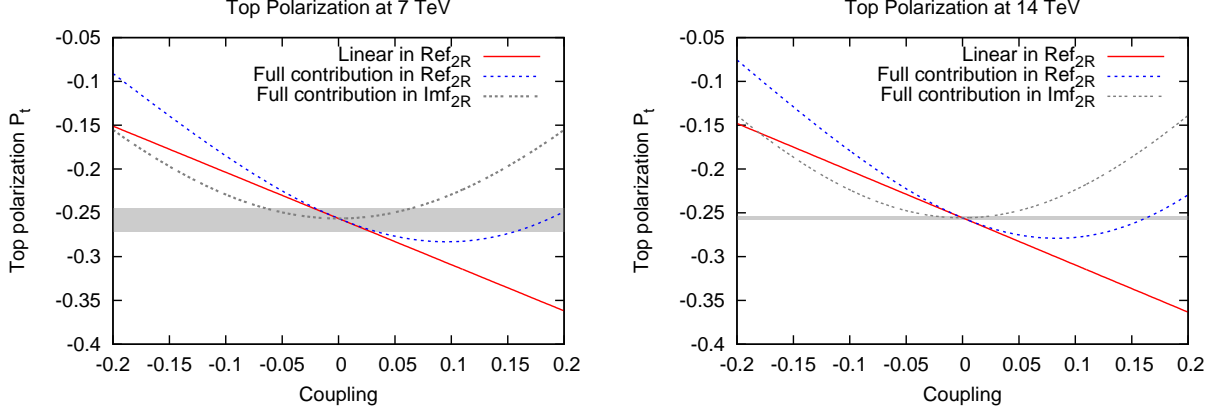


FIG. 6: The top polarization asymmetry for tW^- production at the LHC for two different cm energies, 7 TeV (left) and 14 TeV (right), as a function of anomalous tbW couplings. The grey band corresponds to the top-polarization asymmetry predicted in the SM with a 1σ error interval.

We notice that just as for the total cross section, P_t is more sensitive to negative values of Ref_{2R} . Also, P_t is equally sensitive to negative and positive values of Imf_{2R} . Thus P_t can be a very good probe of Ref_{2R} and Imf_{2R} if it can be measured at the LHC. However, the standard measurement of P_t requires reconstruction of the top rest frame which is a difficult task, and would entail reduction in efficiency. We will therefore investigate lab frame decay distributions for the measurement of anomalous couplings.

All the quantities considered so far, viz., the total cross section, the top polar distribution and the top polarization, can only be measured using information from the decay of the top. Both the polar distribution and the top polarization would play a role in determining the distributions of the decay products. Our main aim is to devise observables which can be measured in the lab frame and give a good estimate of top polarization and thence probe anomalous tbW couplings in single-top production. We proceed to construct such observables from kinematic variables of the charged lepton and b quark produced in the decay of the top.

III. CHARGED-LEPTON DISTRIBUTIONS

Top polarization can be determined by the angular distribution of its decay products. In the SM, the dominant decay mode is $t \rightarrow bW^+$, with a branching ratio (BR) of 0.998, with the W^+ subsequently decaying to $\ell^+\nu_\ell$ (semileptonic decay, BR 1/9 for each lepton) or $u\bar{d}$, $c\bar{s}$ (hadronic decay, BR 2/3). The angular distribution of a decay product f for a top-quark ensemble has the form

$$\frac{1}{\Gamma_f} \frac{d\Gamma_f}{d\cos\theta_f} = \frac{1}{2}(1 + \kappa_f P_t \cos\theta_f). \quad (5)$$

Here θ_f is the angle between fermion f and the top spin vector in the top rest frame and P_t (defined in Eq. 4) is the degree of polarization of the top-quark ensemble. Γ_f is the partial decay width and κ_f is the spin analyzing power of f . Obviously, a larger κ_f makes f a more sensitive probe of the top spin. The charged lepton and the d quark are the best spin analyzers with $\kappa_{\ell^+} = \kappa_{\bar{d}} = 1$, while $\kappa_{\nu_\ell} = \kappa_u = -0.30$ and $\kappa_b = -\kappa_{W^+} = -0.39$, all κ values

being at tree level [34]. Thus the ℓ^+ or d have the largest probability of being emitted in the direction of the top spin and the least probability in the direction opposite to the spin. Since at the LHC, lepton energy and momentum can be measured with high precision, we focus on leptonic decays of the top.

To preserve spin coherence while combining top production with decay, we make use of the spin density matrix formalism. Since $\Gamma_t/m_t \sim 0.008$, we can use the narrow width approximation (NWA) to write the cross section in terms of the product of the $2 \rightarrow 2$ production density matrix ρ and the decay density matrix Γ of the top as

$$\overline{|\mathcal{M}|^2} = \frac{\pi \delta(p_t^2 - m_t^2)}{\Gamma_t m_t} \sum_{\lambda, \lambda'} \rho(\lambda, \lambda') \Gamma(\lambda, \lambda'). \quad (6)$$

where and $\lambda, \lambda' = \pm 1$ denote (the sign of) the top helicity.

The top production spin density matrix $\rho(\lambda, \lambda')$ for process $gb \rightarrow tW^-$ is given in Appendix. We obtain the top decay density matrix $\Gamma(\lambda, \lambda')$ for the process $t \rightarrow bW^+ \rightarrow b\ell^+\nu_\ell$ including anomalous tbW couplings and write it in a Lorentz invariant form. We find

$$\begin{aligned} \Gamma(\pm, \pm) = & g^4 |\Delta(p_W^2)|^2 [m_t^2 - 2(p_t \cdot p_\ell)] \left[|f_{1L}|^2 \left\{ (p_t \cdot p_\ell) \mp m_t(p_\ell \cdot n_3) \right\} \right. \\ & + \text{Re} f_{1L} f_{2R}^* \left\{ m_t m_W \mp \frac{m_t^2 + m_W^2}{m_W} (p_\ell \cdot n_3) \mp \frac{2}{m_W} (p_b \cdot n_3)(p_t \cdot p_\ell) \right\} \\ & \left. + \frac{|f_{2R}|^2}{2} \left\{ m_W^2 + \frac{m_t^2 - 2p_t \cdot p_\ell}{2} \mp 2[(p_\ell \cdot n_3) + (p_b \cdot n_3)] \right\} \right], \end{aligned} \quad (7)$$

for the diagonal elements and

$$\begin{aligned} \Gamma(\mp, \pm) = & g^4 |\Delta(p_W^2)|^2 [m_t^2 - 2(p_t \cdot p_\ell)] \left[|f_{1L}|^2 \left\{ -m_t[p_\ell \cdot (n_1 \mp in_2)] \right\} \right. \\ & - \text{Re} f_{1L} f_{2R}^* \left\{ \frac{m_t^2 + m_W^2}{m_W} [p_\ell \cdot (n_1 \mp in_2)] - \frac{2}{m_W} [p_b \cdot (n_1 \mp in_2)](p_t \cdot p_\ell) \right\} \\ & \left. - |f_{2R}|^2 \left\{ [(p_\ell + p_b) \cdot (n_1 \mp in_2)] \right\} \right], \end{aligned} \quad (8)$$

for the off-diagonal ones. Here $\Delta(p_W^2)$ is the W boson propagator, for which we will use the narrow-width approximations for our numerical calculations, and n_i^μ 's ($i = 1, 2, 3$) are spin four-vectors for the top with four-momentum p_t , corresponding to rest-frame spin quantization axes x , y and z respectively, with the properties $n_i \cdot n_j = -\delta_{ij}$ and $n_i \cdot p_t = 0$. In the top rest frame they take the standard form $n_i^0 = 0$, $n_i^k = \delta_i^k$.

The full details of the factorization of the differential cross section for top production followed by its decay in a generic production process into production and decay parts is given in Ref. [30]. Here we use the same formalism for single-top production and its decay and write the partial cross section in the parton cm of frame as

$$d\sigma = \frac{1}{32(2\pi)^4 \Gamma_t m_t} \int \left[\sum_{\lambda, \lambda'} \frac{d\sigma(\lambda, \lambda')}{d \cos \theta_t} \left(\frac{\langle \Gamma(\lambda, \lambda') \rangle}{p_t \cdot p_\ell} \right) \right] d \cos \theta_t d \cos \theta_\ell d\phi_\ell E_\ell dE_\ell dp_W^2, \quad (9)$$

where the b -quark energy integral is replaced by an integral over the invariant mass p_W^2 of the W boson, its polar-angle integral is carried out using the Dirac delta function of Eq. 6, and the average over its azimuthal angle is denoted by the angular brackets. $d\sigma(\lambda, \lambda')/d \cos \theta_t$ is proportional to $\rho(\lambda, \lambda')$, with the normalization chosen so that $d\sigma(\lambda, \lambda)/d \cos \theta_t$ is the differential cross section for the $2 \rightarrow 2$ process of tW^- production with helicity index λ of the top.

A. Angular distributions of charged leptons

We evaluate top decay in the rest frame of the top quark with the z axis as the spin quantization axis, which would also be the direction of the boost required to go to the parton cm frame. In the rest frame of the top quark, the diagonal and off-diagonal elements of decay density matrix, after averaging over the azimuthal angle of b quark w.r.t. the plane of top and lepton momenta, are given by

$$\begin{aligned} \langle \Gamma(\pm, \pm) \rangle &= g^4 m_t E_\ell^0 |\Delta_W(p_W^2)|^2 (m_t^2 - 2p_t \cdot p_\ell) \left[\left\{ |f_{1L}|^2 + \text{Re} f_{1L} f_{2R}^* \frac{m_t}{p_t \cdot p_\ell} \frac{m_W}{p_t \cdot p_\ell} \right\} (1 \pm \cos \theta_\ell^0) \right. \\ &\quad \left. - |f_{2R}|^2 \left(1 - \frac{m_t^2 + m_W^2}{2p_t \cdot p_\ell} \right) (1 \mp \cos \theta_\ell^0) \pm |f_{2R}|^2 \frac{m_W^2 m_t^2}{2(p_t \cdot p_\ell)^2} \cos \theta_\ell^0 \right], \end{aligned} \quad (10)$$

$$\begin{aligned} \langle \Gamma(\pm, \mp) \rangle &= g^4 m_t E_\ell^0 |\Delta_W(p_W^2)|^2 (m_t^2 - 2p_t \cdot p_\ell) \sin \theta_\ell^0 e^{\pm i\phi_\ell^0} \left[|f_{1L}|^2 + \text{Re} f_{1L} f_{2R}^* \frac{m_t}{p_t \cdot p_\ell} \frac{m_W}{p_t \cdot p_\ell} \right. \\ &\quad \left. + |f_{2R}|^2 \left\{ 1 - \frac{m_t^2 + m_W^2}{2p_t \cdot p_\ell} + \frac{m_W^2 m_t^2}{2(p_t \cdot p_\ell)^2} \right\} \right], \end{aligned} \quad (11)$$

where averaging over the azimuthal angle of the b quark w.r.t. the plane of top and lepton momenta, denoted by angular brackets, is most conveniently carried out in a coordinate system defined with the z axis along the lepton momentum direction.

In the limit of small anomalous coupling f_{2R} , we see from Eqs. 10 and 11 that if we drop quadratic terms in f_{2R} , $\langle \Gamma(\lambda, \lambda') \rangle$ factorizes into a pure angular part $\mathcal{A}(\lambda, \lambda')$, which depends on helicities, and a lepton-energy dependent part which does not depend on the helicities, where

$$\mathcal{A}(\pm, \pm) = (1 \pm \cos \theta_\ell^0), \quad \mathcal{A}(\pm, \mp) = \sin \theta_\ell^0 e^{\pm i\phi_\ell^0}. \quad (12)$$

The factorization of $\langle \Gamma(\lambda, \lambda') \rangle$ into $\mathcal{A}(\lambda, \lambda')$ and a helicity-independent part in the rest frame of the top quark implies that since the corrections from anomalous couplings reside in the helicity-independent part, they are identical to those of the total width appearing in the denominator of the angular distribution, and cancel. This leads to the result of [29, 30] that the energy averaged lepton angular distributions are insensitive to the new physics in top-quark decay in any top production process.

We study the angular distribution of the charged lepton in the lab frame both in the linear approximation of the anomalous couplings as well as with full contributions of the anomalous couplings without approximation.

We first obtain the angular distribution of the charged lepton in the parton cm frame, by integrating over the lepton energy, with limits given by $m_W^2 < 2(p_t \cdot p_\ell) < m_t^2$. This integral can be done analytically, giving the following expression for the differential cross section in the parton cm frame:

$$\frac{d\sigma}{d \cos \theta_t \, d \cos \theta_\ell \, d\phi_\ell} = \frac{1}{32 \, \Gamma_t m_t} \frac{1}{(2\pi)^4} \int \left[\sum_{\lambda, \lambda'} \frac{d\sigma(\lambda, \lambda')}{d \cos \theta_t} g^4 \mathcal{A}'(\lambda, \lambda') \right] |\Delta(p_W^2)|^2 dp_W^2, \quad (13)$$

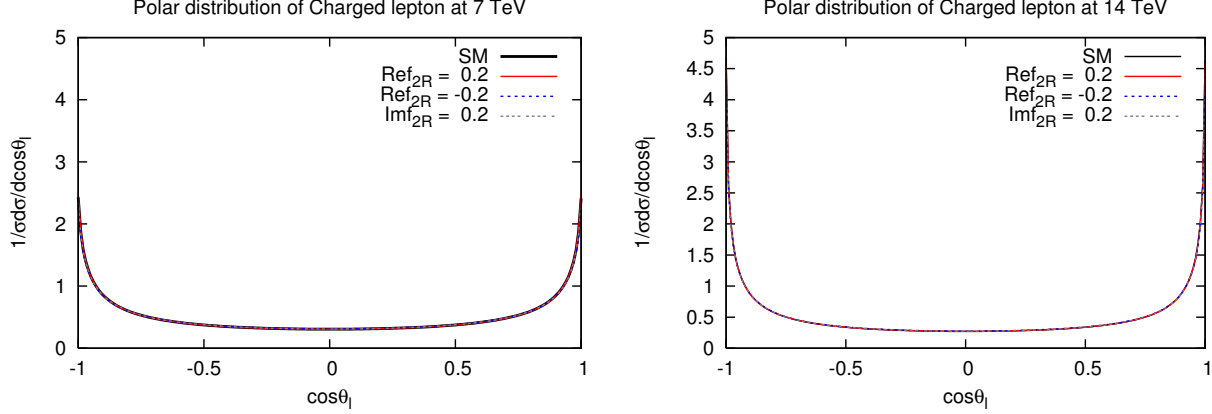


FIG. 7: The normalized polar distribution of the charged lepton in tW^- production at the LHC for two different cm energies, 7 TeV (left) and 14 TeV (right), for different anomalous tbW couplings.

where

$$\begin{aligned} \mathcal{A}'(\pm, \pm) &= \frac{m_t^6}{24(1 - \beta_t \cos \theta_{t\ell})^3 E_t^2} \left[(1 - r^2)^2 \{ (1 \pm \cos \theta_{t\ell})(1 \mp \beta_t) [|f_{1L}|^2(1 + 2r^2) + 6r \text{Ref}_{1L} f_{2R}^*] \right. \\ &\quad + |f_{2R}|^2(2 + r^2)(1 \mp \cos \theta_{t\ell})(1 \pm \beta_t) \} \\ &\quad \mp 12r^2 |f_{2R}|^2 (1 - r^2 + 2 \log r) (\cos \theta_{t\ell} - \beta_t) \Big], \end{aligned} \quad (14)$$

$$\begin{aligned} \mathcal{A}'(\pm, \mp) &= \frac{m_t^7}{24(1 - \beta_t \cos \theta_{t\ell})^3 E_t^3} \sin \theta_{t\ell} e^{\pm i \phi_\ell} \left[(1 - r^2)^2 \{ |f_{1L}|^2(1 + 2r^2) + 6r \text{Ref}_{1L} f_{2R}^* \right. \\ &\quad \left. - |f_{2R}|^2(2 + r^2) \} - 12r^2 |f_{2R}|^2 (1 - r^2 + 2 \log r) \right]. \end{aligned} \quad (15)$$

Here $r = m_W/m_t$ and $\cos \theta_{t\ell}$ is the angle between the top quark and the charged lepton from the top decay in the parton cm frame, given by

$$\cos \theta_{t\ell} = \cos \theta_t \cos \theta_\ell + \sin \theta_t \sin \theta_\ell \cos \phi_\ell, \quad (16)$$

where θ_ℓ and ϕ_ℓ are the lepton polar and azimuthal angles.

In the lab frame, the lepton polar angle is defined w.r.t. either of the beam direction and the azimuthal angle is defined with respect to the top-production plane chosen as the x - z plane, with beam direction as the z axis and the convention that the x component of the top momentum is positive. At the LHC, which is a symmetric collider, it is not possible to define a positive direction of the z axis. Hence lepton angular distribution is symmetric under interchange of θ_ℓ and $\pi - \theta_\ell$ as well as of ϕ_ℓ and $2\pi - \phi_\ell$. The lab frame expression for the differential cross section is obtained from Eq. 13 by an appropriate Lorentz transformation and integration over the parton densities.

We first look at the polar distribution of the charged lepton and the effect on it of anomalous tbW couplings. As can be seen from Fig. 7, where we plot the polar distribution for two cm of the LHC energies $\sqrt{s} = 7$ TeV and 14 TeV, the normalized distributions are insensitive to anomalous tbW couplings.

We next look at the contributions of anomalous couplings to the azimuthal distribution of the charged lepton. In Fig. 8, we show the normalized azimuthal distribution of the

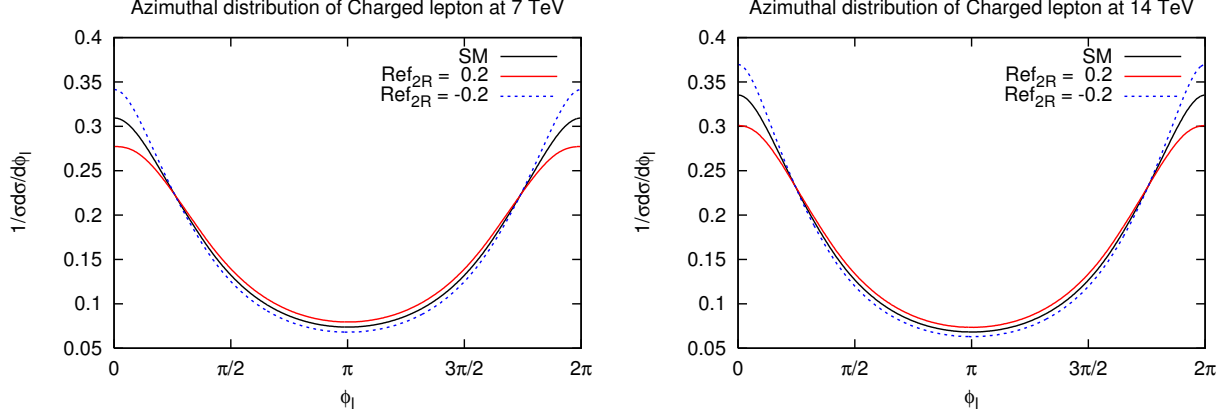


FIG. 8: The normalized azimuthal distribution of the charged lepton in tW^- production at the LHC for two different cm energies, 7 TeV (left) and 14 TeV (right), for different anomalous tbW couplings in the linear approximation. $\text{Im}f_{2R}$ does not contribute in the linear order.

charged lepton in a linear approximation of the couplings for $\sqrt{s} = 7$ TeV and 14 TeV for different values of $\text{Re}f_{2R}$. At linear order, contributions of all other couplings vanish in the limit of vanishing bottom mass. In Fig. 9, we show the normalized azimuthal distribution of the charged lepton including higher-order terms in the couplings for $\sqrt{s} = 7$ TeV and 14 TeV for different values of $\text{Re}f_{2R}$ and $\text{Im}f_{2R}$. We see that the curves for real and imaginary parts of the anomalous coupling f_{2R} peak near $\phi_\ell = 0$ and $\phi_\ell = 2\pi$. The curves are well

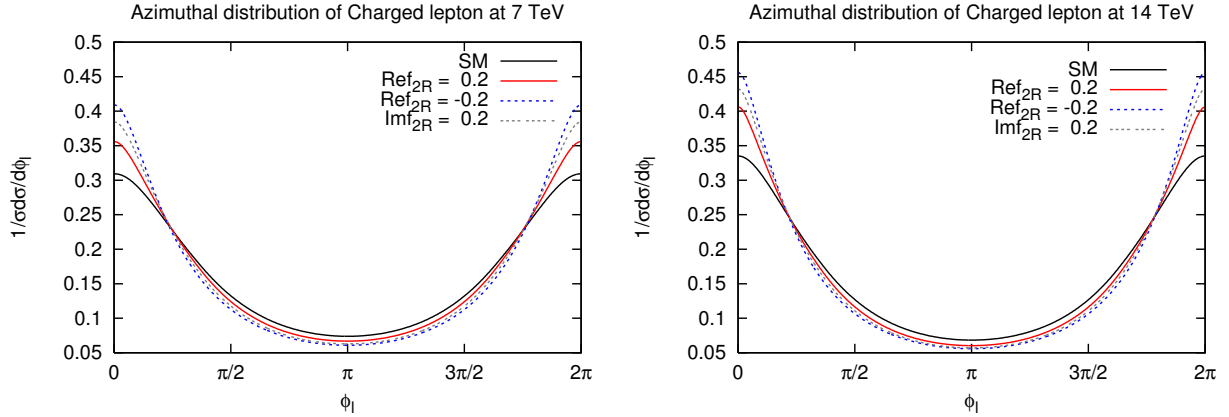


FIG. 9: The normalized azimuthal distribution of the charged lepton in tW^- production at the LHC for two different cm energies, 7 TeV (left) and 14 TeV (right), for different anomalous tbW couplings without the linear approximation

separated at the peaks for the chosen values of the anomalous tbW couplings and are also well separated from the curve for the SM. We define an azimuthal asymmetry for the lepton to quantify these differences in the distributions by

$$A_\phi = \frac{\sigma(\cos \phi_\ell > 0) - \sigma(\cos \phi_\ell < 0)}{\sigma(\cos \phi_\ell > 0) + \sigma(\cos \phi_\ell < 0)}, \quad (17)$$

where the denominator is the total cross section. Plots of A_ϕ as a function of the couplings

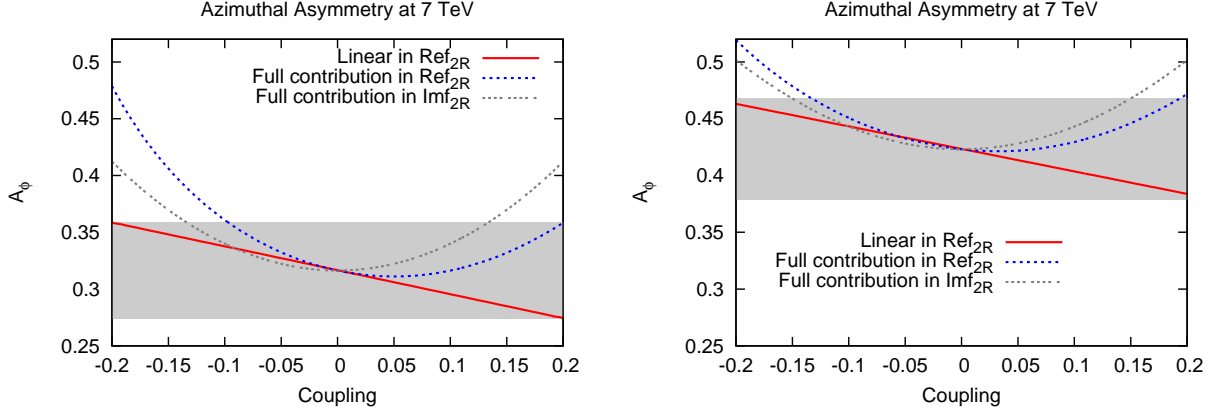


FIG. 10: The azimuthal asymmetries of the charged lepton in tW^- production at the LHC for cm energy 7 TeV without lepton cuts (left) and with cuts (right), as a function of anomalous tbW couplings. The grey band corresponds to the azimuthal asymmetry predicted in the SM with 1σ error interval.

with and without cuts on the lepton momenta are shown in Fig. 10 for a cm energy of 7 TeV. In the former case, the rapidity and transverse momentum acceptance cuts on the decay lepton that we have used are $|\eta| < 2.5$, $p_T^\ell > 20$ GeV. The corresponding plots at $\sqrt{s} = 14$

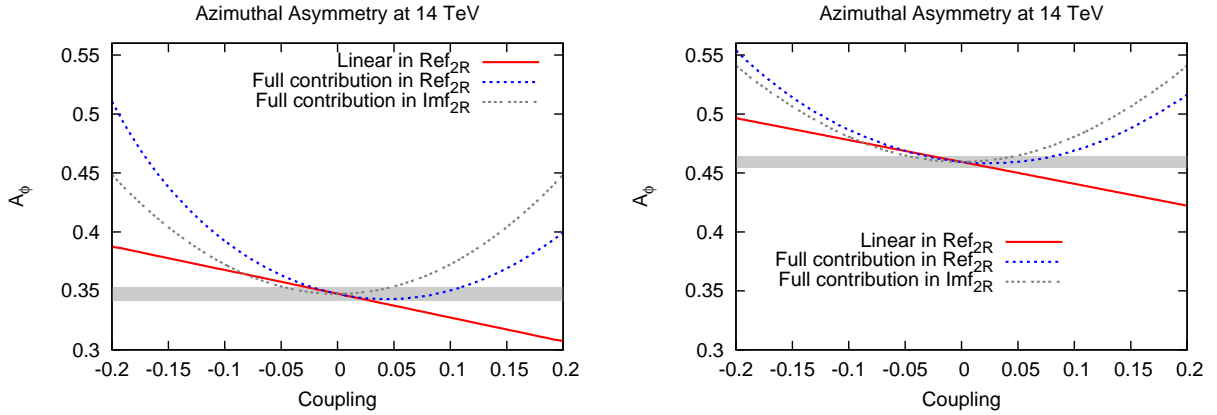


FIG. 11: The azimuthal asymmetries of the charged lepton in tW^- production at the LHC for cm energy 14 TeV without lepton cuts (left) and with cuts (right), as a function of anomalous tbW couplings. The grey band corresponds to the azimuthal asymmetry predicted in the SM with a 1σ error interval.

TeV with and without lepton cuts are shown in the Fig. 11. The lepton cuts increase the value of A_ϕ for the SM from 0.35 to around 0.45, and also increase A_ϕ substantially with anomalous couplings included. However, the cuts result in the reduction of signal events and from the Figs. 10 and 11, we see that these cuts actually decrease the sensitivity to anomalous couplings.

The azimuthal distribution depends both on top polarization and on a kinematic effect. According to Eq. 5, the decay lepton is emitted preferentially along the top spin direction in the top rest frame, with $\kappa_f = 1$. The corresponding distributions in the parton cm frame are given by Eq. 13 with the angular parts described by Eqs. 14 and 15. The rest-frame forward (backward) peak corresponds to a peak for $\cos\theta_{t\ell} = \pm 1$, as seen from the factor $(1 \pm \cos\theta_{t\ell})$ in the numerator of Eq. 14. This is the effect of polarization. The kinematic effect is seen in the factor $(1 - \beta_t \cos\theta_{t\ell})^3$ in the denominator of Eqs. 14 and 15, which again gives rise to peaking for large $\cos\theta_{t\ell}$. Eq. 16 therefore implies peaking for small ϕ_ℓ . This is borne out by the numerical results.

B. Energy distribution of charged leptons

We now study the energy distribution $d\sigma/dE_\ell$ of charged leptons to probe anomalous tbW couplings in single-top production and decay. In the rest frame of the top quark, the E_ℓ distribution of the decay density matrix $\Gamma(\lambda, \lambda')$ depends only on the combination of helicities, (λ, λ') . To linear order in the couplings, only the angular part of $\Gamma(\lambda, \lambda')$ depends on the helicities, and the energy dependence is the same for all helicity combinations, and is determined by the effective couplings occurring in decay. However, there is a weak dependence on the production differential cross section introduced because the boost to the parton cm frame is determined by $\theta_{t\ell}$. Thus, the E_ℓ distribution arises mainly from the decay process, and depends only weakly on the polarization.

We plot in Fig. 12 the E_ℓ distribution for $\sqrt{s} = 7$ and 14 TeV. We see that the distribution

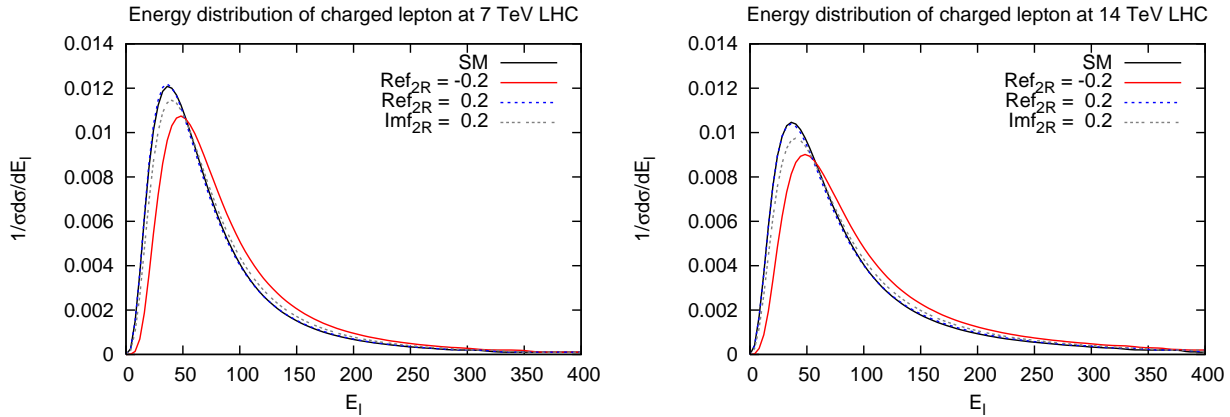


FIG. 12: The energy distribution of the charged lepton in tW^- production at the LHC for cm energies 7 TeV (left) TeV and 14 TeV (right) for different anomalous tbW couplings.

is peaked at low values of E_ℓ around 40-45 GeV, and all curves intersect at a particular value of $E_\ell \approx 62$ GeV. We also observe that the E_ℓ distribution is mainly sensitive to Ref_{2R} .

As seen from Fig. 12, the E_ℓ distribution is very sensitive to negative values of Ref_{2R} and shows little sensitivity for positive values. The E_ℓ distribution at 7 TeV is peaked slightly more as compared to that for 14 TeV LHC, though the position of the peak for both is about the same.

The curves for the E_ℓ distribution for anomalous tbW couplings of ± 0.2 and the SM are well separated from each other and intersect at $E_\ell^C = 62$ GeV. To quantify this difference

and to make better use of statistics, we construct an asymmetry around the intersection point of the curves, defined by

$$A_{E_\ell} = \frac{\sigma(E_\ell < E_\ell^C) - \sigma(E_\ell > E_\ell^C)}{\sigma(E_\ell < E_\ell^C) + \sigma(E_\ell > E_\ell^C)}, \quad (18)$$

where the denominator is the total cross section. Plots for A_{E_ℓ} as a function the coupling

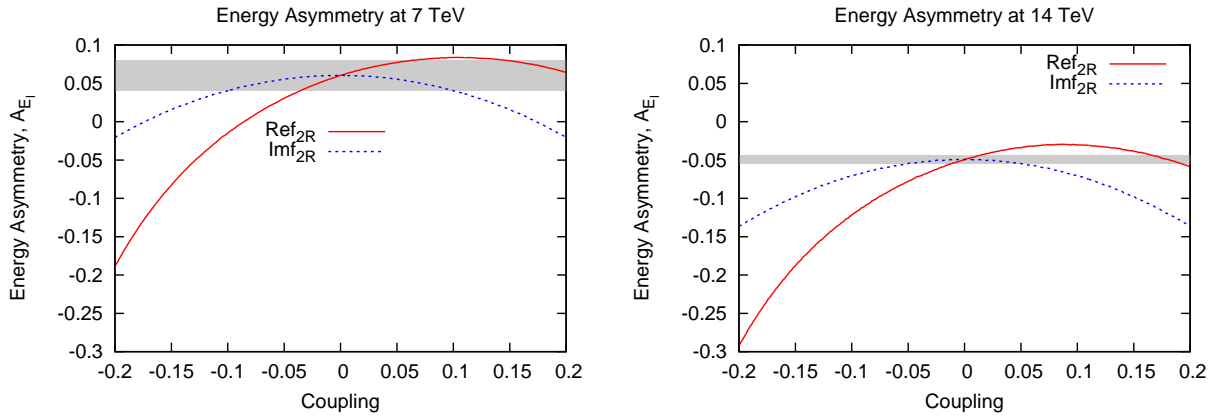


FIG. 13: The energy asymmetry of the charged lepton in tW^- production at the LHC for cm energy 14 TeV without lepton cuts (left) and with cuts (right), as a function of anomalous tbW couplings. The grey band corresponds to the energy asymmetry predicted in the SM with a 1σ error interval.

are shown in Fig. 13 for two cm energies of 7 TeV and 14 TeV. We can see from the figure that A_{E_ℓ} is very sensitive to Ref_{2R} and hence can be a sensitive probe of this coupling. It is also seen from the figure that the A_{E_ℓ} for the SM is positive for $\sqrt{s} = 7$ TeV, but negative for $\sqrt{s} = 14$ TeV. This is in accordance with a sharper peaking of the energy distribution in the former case. Another difference between the asymmetries for the two cm energies is that A_{E_ℓ} changes sign with the sign for some value of Ref_{2R} in case of $\sqrt{s} = 7$ TeV, but remains negative in case of $\sqrt{s} = 14$ TeV.

IV. ANGULAR DISTRIBUTION OF b QUARKS

Although the charged-lepton azimuthal distribution provides a neat way to probe top polarization independent of new physics in the top-decay vertex, it suffers from low branching ratio of W and hence low number of events for the analysis. This situation can be improved upon by using b -quark angular distributions, without restricting only to the leptonic decays of the W coming from top decay, and thus utilizing all the single-top events. We thus assume, for purposes of this section, that the top quark can be identified in hadronic and semi-leptonic decays with sufficiently good efficiency to enable measurement of b -quark distribution in all of them.

As described earlier, we use NWA to factorize the full process into single-top production and top decay. Similar to Eq. 9, we can write the full differential cross section for the

process $g(p_g)b(p_b) \rightarrow t(p_t, \lambda_t)W^-$ followed by $t(p_t, \lambda_t) \rightarrow b(p'_b)W^+$ as

$$\frac{d\sigma}{d\cos\theta_t d\Omega_b} = \frac{1}{128(2\pi)^3 \hat{s}^{3/2}} \frac{|\vec{p}_t|}{\Gamma_t m_t} \frac{(m_t^2 - m_W^2)}{E_t^2 (1 - \beta_t \cos\theta_{bt})^2} \sum_{\lambda_t, \lambda'_t} [\rho(\lambda_t, \lambda'_t) \Gamma(\lambda_t, \lambda'_t)], \quad (19)$$

where the polar angle θ_t of the top quark, and the polar and azimuthal angles θ_b and ϕ_b of the b quark produced in top decay, are measured with respect to the parton direction as the z axis, and with the xz plane defined as the plane containing the top momentum. θ_{bt} is the angle between the top momentum and the momentum of the decay b quark.

The density matrix for single-top production $\rho(\lambda_t, \lambda'_t)$ appearing in Eq. 19 is given in the Appendix. The decay density matrix for $t \rightarrow bW$ in the top-quark rest frame is given by [43]

$$\Gamma(\pm, \pm) = \frac{g^2 m_t^2}{2} [\mathcal{C}_1 \pm \mathcal{C}_2 \cos\theta_b^0], \quad (20)$$

$$\Gamma(\pm, \mp) = \frac{g^2 m_t^2}{2} [\mathcal{C}_2 \sin\theta_b^0 e^{\pm\phi_b^0}], \quad (21)$$

where

$$\mathcal{C}_1 = \frac{1}{2r^2} (1 - r^2) [|\mathbf{f}_{1L}|^2 (2r^2 + 1) + \text{Re} \mathbf{f}_{1L} \mathbf{f}_{2R}^* 6r + |\mathbf{f}_{2R}|^2 (2 + r^2)], \quad (22)$$

$$\mathcal{C}_2 = \frac{1}{2r^2} (1 - r^2) [|\mathbf{f}_{1L}|^2 (2r^2 - 1) + \text{Re} \mathbf{f}_{1L} \mathbf{f}_{2R}^* 2r + |\mathbf{f}_{2R}|^2 (2 - r^2)]. \quad (23)$$

The rest frame polar and azimuthal angles of the b , respectively θ_b^0 and ϕ_b^0 , may be expressed in terms of the parton cm frame angles in a straightforward way.

Plots for the azimuthal distribution of the b quark for different values of anomalous couplings $\text{Re} \mathbf{f}_{2R}$ and $\text{Im} \mathbf{f}_{2R}$ are shown in Fig. 14. The curves for values ± 0.2 of these couplings are well separated from each other and from the SM curve. In the azimuthal distribution of the b quark, we get dependence on anomalous couplings both from production as well as decay. We find that the contributions from production and from decay come with opposite signs, partially cancelling each other.

To study the sensitivity and make the best use of azimuthal b -quark distribution, we construct an asymmetry A_b :

$$A_b = \frac{\sigma(\cos\phi_b > 0) - \sigma(\cos\phi_b < 0)}{\sigma(\cos\phi_b > 0) + \sigma(\cos\phi_b < 0)}. \quad (24)$$

The asymmetry A_b is plotted in Fig. 15 as a function of anomalous couplings for the cm energies $\sqrt{s} = 7$ TeV and 14 TeV. From the figure it is clear that A_b shows less sensitivity to couplings $\text{Re} \mathbf{f}_{2R}$ and $\text{Im} \mathbf{f}_{2R}$ as compared to other asymmetries. As stated earlier, this is due to the fact that the contributions of anomalous couplings to the asymmetry from the production and the decay are of opposite in sign and hence tend to cancel each other.

V. SENSITIVITY ANALYSIS FOR ANOMALOUS tbW COUPLINGS

We now study the sensitivities of the observables discussed in the previous sections to the anomalous tbW couplings at the LHC running at two cm of energies viz., 7 TeV and 14 TeV,

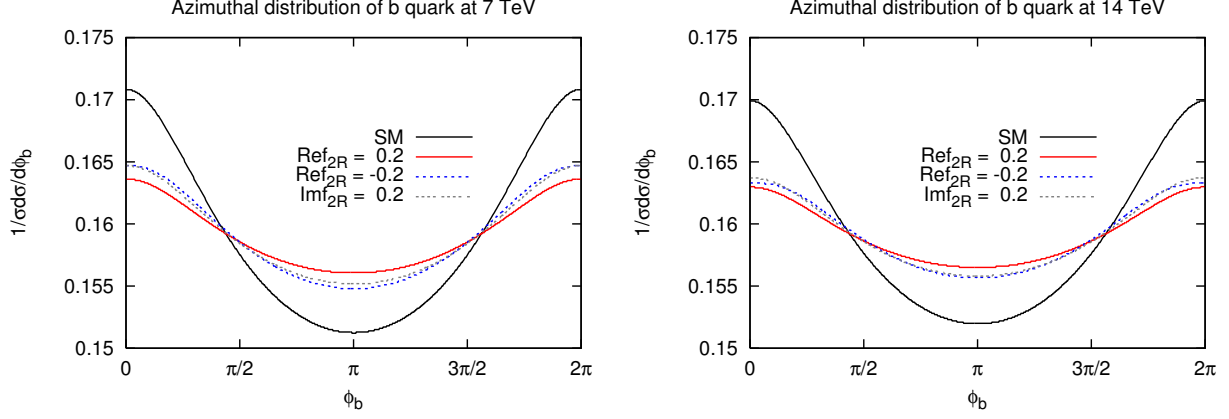


FIG. 14: The azimuthal distribution of the b quark in tW^- production at the LHC for cm energies 7 TeV and 14 TeV for different anomalous tbW couplings.

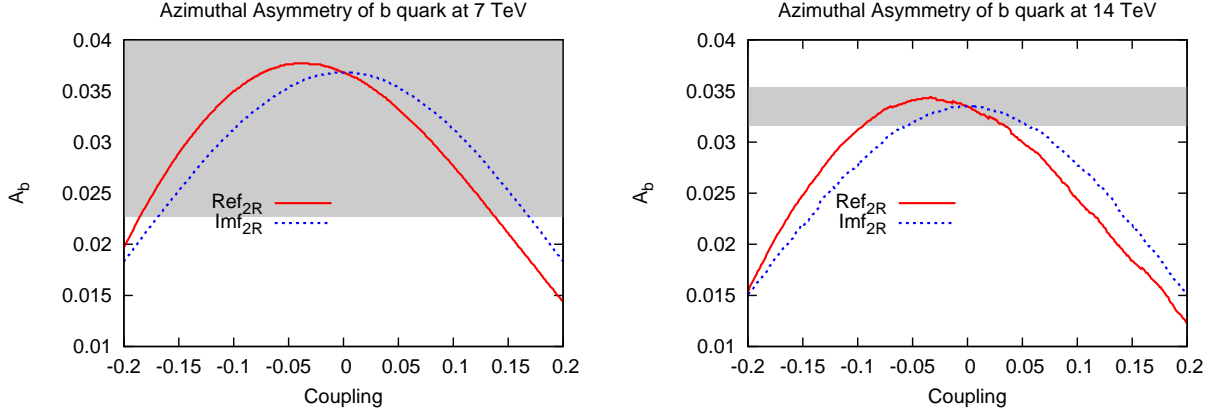


FIG. 15: The azimuthal asymmetry of the b quark in tW^- production at the LHC for cm energies 7 TeV and 14 TeV as a function of anomalous tbW couplings. The grey band corresponds to the asymmetry predicted in the SM with a 1σ error interval.

with integrated luminosities 1 fb^{-1} and 10 fb^{-1} , respectively. To obtain the 1σ limit on the anomalous tbW couplings from a measurement of an observable, we find those values of the couplings for which observable deviates by 1σ from its SM value. The statistical uncertainty σ_i in the measurement of any generic asymmetry \mathcal{A}_i is given by

$$\sigma_i = \sqrt{\frac{1 - (\mathcal{A}_i^{SM})^2}{\mathcal{N}}}, \quad (25)$$

where \mathcal{A}_i^{SM} is the asymmetry predicted in the SM and \mathcal{N} is the total number of events predicted in the SM. We apply this to the various asymmetries we have discussed. In case of the top polarization asymmetry, the limits are obtained on the assumption that the polarization can be measured with 100% accuracy.

The 1σ limits on Ref_{2R} and Imf_{2R} are given in Table I where we assume only one anomalous coupling to be non-zero at a time. We have also assumed measurements on a tW^- final

state. Including the $\bar{t}W^+$ final state will improve the limits by a factor of $\sqrt{2}$. In case of the lepton distributions, we take into account only one leptonic channel. Again, including other leptonic decays of the top would improve the limits further. The limits corresponding to a linear approximation in the couplings are denoted by the label “lin. approx.”. Apart from the 1σ limits shown in Table I, which correspond to intervals which include zero value of the coupling, there are other disjoint intervals which could be ruled out by null if no deviation from the SM is observed for P_t and A_{E_ℓ} . This is apparent from Figs. 6 and 13. The additional allowed intervals for Ref_{2R} from P_t measurement are $[0.158, 0.205]$ and $[0.160, 0.167]$ for cm energies of 7 TeV and 14 TeV, respectively. The corresponding intervals for A_{E_ℓ} are $[0.147, 0.285]$ and $[0.175, 0.185]$ [44].

	7 TeV		14 TeV	
Observable	Ref_{2R}	Imf_{2R}	Ref_{2R}	Imf_{2R}
P_t	$[-0.025, 0.032]$	$[-0.072, 0.072]$	$[-0.004, 0.004]$	$[-0.034, 0.034]$
P_t (lin. approx.)	$[-0.027, 0.027]$	—	$[-0.004, 0.004]$	—
A_ϕ	$[-0.133, 0.194]$	$[-0.150, 0.150]$	$[-0.034, 0.086]$	$[-0.050, 0.050]$
A_ϕ (lin. approx.)	$[-0.204, 0.204]$	—	$[-0.030, 0.030]$	—
A_b	$[-0.191, 0.147]$	$[-0.177, 0.177]$	$[-0.096, 0.035]$	$[-0.059, 0.059]$
A_{E_ℓ}	$[-0.044, 0.073]$	$[-0.114, 0.114]$	$[-0.006, 0.009]$	$[-0.038, 0.038]$

TABLE I: Individual limits on real and imaginary parts of anomalous coupling f_{2R} which may be obtained by the measurement of the observables shown in the first column of the table at two cm of energies viz., 7 TeV and 14 TeV with integrated luminosities of 1 fb^{-1} and 10 fb^{-1} respectively. A dash “—” indicates that no limits are possible.

It is seen that the azimuthal asymmetry A_ϕ and the energy asymmetry A_{E_ℓ} of the charged lepton are more sensitive to negative values of the anomalous couplings Ref_{2R} . A_{E_ℓ} is the most sensitive of the asymmetries we consider. In fact, the sensitivity of A_{E_ℓ} to Ref_{2R} and Imf_{2R} is comparable to the sensitivity of top polarization to the same couplings, despite the fact that only one leptonic decay channel, with a branching fraction of about $1/9$, is considered for A_{E_ℓ} . The additional contribution to A_{E_ℓ} of the f_{2R} coupling through the top decay channel seems to compensate for the low branching fraction. A_b is seen to have the lowest sensitivity, where there is partial cancellation of contributions to the asymmetry from production and from decay.

We also obtain simultaneous limits (taking both Ref_{2R} and Imf_{2R} non-zero simultaneously) on these anomalous couplings that may be obtained by combining the measurements of all observables. For this, we perform a χ^2 analysis to fit all the observables to within $f\sigma$ of statistical errors in the measurement of the observable. We define the following χ^2 function

$$\chi^2 = \sum_{i=1}^n \left(\frac{P_i - O_i}{\sigma_i} \right)^2, \quad (26)$$

where the sum runs over the n observables measured and f is the degree of the confidence interval. P_i ’s are the values of the observables obtained by taking both anomalous couplings non-zero (and is a function of the couplings Ref_{2R} and Imf_{2R}) and O_i ’s are the values of the observables obtained in the SM. σ_i ’s are the statistical fluctuations in the measurement of the observables, given in Eq. 25.

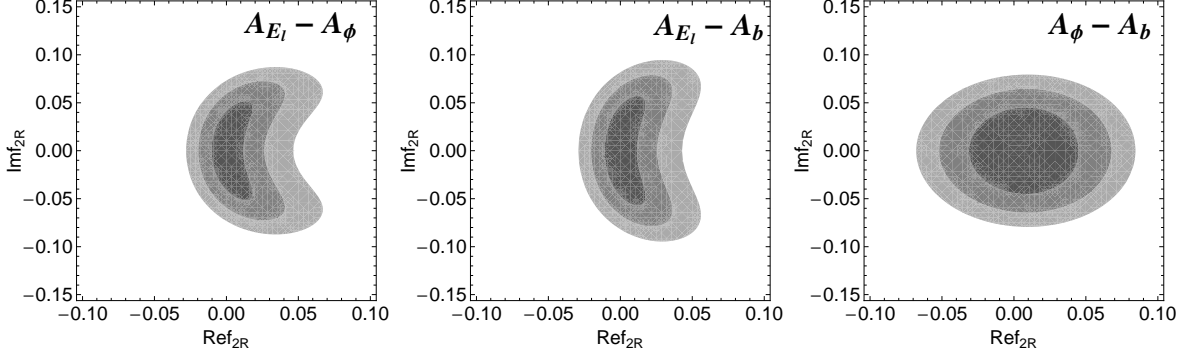


FIG. 16: The 1σ (central region), 2σ (middle region) and 3σ (outer region) CL regions in the Ref_{2R} - Imf_{2R} plane allowed by the combined measurement of two observables at a time. The left, centre and right plots correspond to measurements of the combinations $A_{E_\ell}-A_\phi$, $A_{E_\ell}-A_b$ and $A_\phi-A_b$ respectively. The χ^2 values for 1σ , 2σ and 3σ CL intervals are 2.30, 6.18 and 11.83 respectively for 2 parameters in the fit.

In Fig. 16, we show the 1σ , 2σ and 3σ regions in Ref_{2R} - Imf_{2R} plane allowed by combined measurement of asymmetries A_{E_ℓ} , A_ϕ and A_b taken two at a time. For this, in the χ^2 function of Eq. 26, we have taken only two of the three observables at a time. From among the three combinations shown in Fig. 16, we find that the strongest simultaneous limits come from the combined measurement of A_{E_ℓ} and A_ϕ , viz., $[-0.01, 0.02]$ on Ref_{2R} and $[-0.05, 0.05]$ on Imf_{2R} , at the 1σ level.

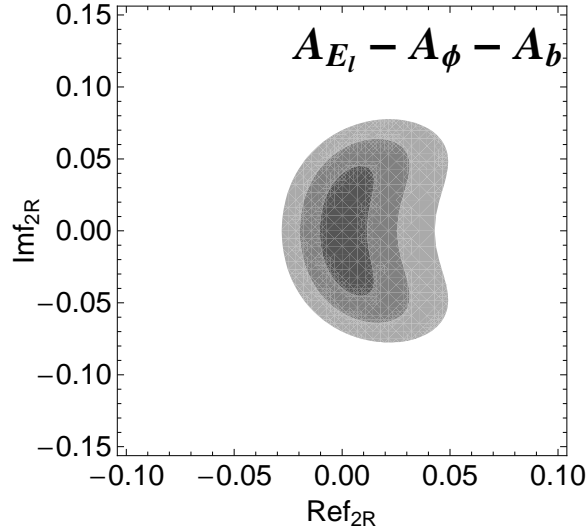


FIG. 17: The 1σ (central region), 2σ (middle region) and 3σ (outer region) CL regions in the Ref_{2R} - Imf_{2R} plane allowed by the combined measurement of all the observables simultaneously.

In Fig. 17, we show the 1σ , 2σ and 3σ regions in Ref_{2R} - Imf_{2R} plane allowed by combined measurement of all three asymmetries A_{E_ℓ} , A_ϕ and A_b simultaneously. We find that the combined measurement of all the observables provide the most stringent simultaneous limits

on $\text{Re}f_{2R}$ and $\text{Im}f_{2R}$ of $[-0.010, 0.015]$ and $[-0.04, 0.04]$ respectively at 1σ . We find that the energy asymmetry A_{E_ℓ} plays a crucial role in determining the combined limits.

We now compare our results with those of other works on the determination of anomalous tbW couplings at the LHC. Refs. [12, 14, 15, 21, 37–39], have studied single-top production at the LHC in the context of anomalous tbW couplings. Boos et al. [12] find a limit of $0.12 < f_{2R} < 0.13$ at the LHC with 100 fb^{-1} of luminosity. Refs. [14, 15] considered couplings f_{1L} and f_{1R} in their analysis and ignored f_{2R} on which we focus. In Ref. [37], the authors have studied all three single-top production channels to probe anomalous tbW couplings and have utilized combinations of observables like cross sections, W polarization helicity fractions in top decay, and other angular asymmetries. They predict a 1σ limit of $[-0.012, 0.024]$ on the coupling f_{2R} with an integrated luminosity of 30 fb^{-1} . Ref. [38] determine expected 3σ limits on $\text{Re}f_{2R}$ to be $[-0.056, 0.056]$ and on $\text{Im}f_{2R}$ to be $[-0.115, 0.115]$, with 10 fb^{-1} of integrated luminosity. Najafabadi [39] has studied the tW channel for single-top production and determined the expected 1σ CL limits on anomalous coupling f_{2R} to be in the range $[-0.026, 0.017]$ with 20 fb^{-1} of integrated luminosity at 14 TeV LHC using the single-top production cross section.

Refs. [23, 35, 36] have studied various observables in $t\bar{t}$ pair production at the LHC with semileptonic decays of the top. Ref. [23] predict 1σ limit on f_{2R} of $[-0.019, 0.018]$ with 10 fb^{-1} of integrated luminosity. Refs. [35, 36] study W polarization in top decay in top-quark pair production at the LHC to constrain the anomalous tbW couplings. They construct various asymmetries and helicity fractions to probe anomalous couplings in the decay of the top quark. Ref. [35] quotes a 2σ limit of 0.04 on f_{2R} with full detector-level simulations including systematic uncertainties and with different observables. Ref. [36] obtain a limit on f_{2R} of $[-0.0260, 0.0312]$ with simulation of the ATLAS detector.

All these analyses except those of [23, 38] consider anomalous tbW couplings to be real parameters. In our analysis, we consider all anomalous couplings to be complex and find that only the real part of the coupling f_{2R} gives significant contribution to all observables at linear order in anomalous couplings. Without a linear approximation, other couplings also contributes at the quadratic level. However, we focus only on the f_{2R} since its contribution is dominant, occurring as it does at linear order. With integrated luminosity 10 fb^{-1} and cm energy 14 TeV, we find the most stringent limits possible on $\text{Re}f_{2R}$ to be $[-0.006, 0.009]$ and on $\text{Im}f_{2R}$ to be $\pm 3.8 \times 10^{-2}$, coming from the lepton energy asymmetry A_{E_ℓ} , which are nominally an order of magnitude better than the Tevatron direct search limit and better than the limits obtained in Refs. [12, 23, 35–38]. Our estimate $[-0.044, 0.073]$ for limits on $\text{Re}f_{2R}$ in the $\sqrt{s} = 7 \text{ TeV}$ run is comparable to the numbers obtained by the extrapolation of the result of [21] to an integrated luminosity of 1 fb^{-1} . It is of course true that including realistic detector efficiencies, especially for b tagging, will worsen our limits somewhat. But, the crucial point in our analysis is that we are able to determine limits on real and imaginary parts of coupling f_{2R} separately while others determine limits only on the magnitude of f_{2R} .

VI. BACKGROUNDS AND NEXT-TO-LEADING-ORDER CORRECTIONS

It is worthwhile to examine the dominant backgrounds to our signal process $gb \rightarrow tW^-$. Background estimation and extraction of the signal for this process has been studied in detail in Refs. [13, 40]. The main background for this signal would come from (a) processes which contain continuum of W^+W^-b involving an off-shell top quark, (b) top-pair production where one of the b quarks is missed as it lies outside the detector range, (c) processes containing

W^+W^-j where lighter-quark jet j is misidentified as a b -quark jet (the probability being 1%). The contributions of the processes W^+W^-b and W^+W^-j , which are of order $O(\alpha_s\alpha_W^2)$, are much smaller than the tW^- signal, which is of order $O(\alpha_s\alpha_W)$. Tait [13] has considered both W 's to decay leptonically and hence the final state consists of two hard charged leptons + one b jet + missing E_T (arising from two neutrinos). For such a signal, the process ZZj would also act as background where one of the Z decays into a pair of the charged leptons and the other Z decays into neutrinos. In Ref. [13], all the backgrounds are simulated at LO in the strong and weak couplings and standard acceptance cuts ($p_T > 15$ GeV and $\eta < 2$) are applied on all final state particles. To suppress large $t\bar{t}$ background, it is required that there should not be more than one hard b jet. After applying these cuts and with integrated luminosity less than 1 fb^{-1} at 14 TeV LHC, the conclusion of the Ref. [13] is that 5σ observation of single-top events in tW^- channel is possible.

The authors of Ref. [40] consider the situation where the W coming from the top quark decays leptonically and the other W decays into two light-quark jets. Therefore the signal would consist of three jets, one of which is a hard b jet, an isolated hard charged lepton and missing energy. The jet multiplicity requirement rejects a major part of the $t\bar{t}$ background. Also, the requirement of the two-jet invariant mass to be within the vicinity of the W mass (70 GeV-90 GeV) eliminates all backgrounds which do not have another W , as for example W +jets, other single-top and QCD processes. In all these analyses, b -tagging efficiency is assumed to be 60%. After applying all the cuts, it has been shown that 10% sensitivity can be achieved with 1 fb^{-1} by combining both electron and muon channels.

Turning to radiative corrections, NLO QCD corrections to the process $gb \rightarrow tW^-$ in the context of the 14 TeV LHC has been studied in detail in Ref. [41]. These corrections are substantial, up to 70% of the LO cross section. They are shown to be dependent on the factorization scale and increase steadily with the increment in the scale. For factorization scale $\mu = \mu_0/2 = (m_t + m_W)/2$, the K factor for the QCD correction is 1.4 while for $\mu = 2\mu_0 = 2(m_t + m_W)$, it is around 1.7. In our analysis, we have taken $\mu = m_t$, for which the K factor is expected to be about 1.5.

The complete NLO EW corrections have been calculated in Ref. [42] for $pp \rightarrow tW^- + X$ in the context of the LHC. The EW corrections are always positive and are maximum for tW invariant mass closed to threshold value. With the increase in tW invariant mass, these EW corrections decrease. So, the maximum EW correction is around 7% at threshold and it goes down to 3.5% for tW invariant mass of 1200 GeV.

In our analysis, we have not included any K factor. Including NLO factors in our analysis would not change the asymmetries much, but would increase the signal and hence, the sensitivity on anomalous couplings would be enhanced.

VII. SUMMARY AND CONCLUSIONS

We have investigated the sensitivity of the LHC to anomalous tbW couplings in single-top production in association with a W^- boson followed by semileptonic decay of the top. We derived analytical expressions for the spin density matrix of the top quark including contributions of both real and imaginary parts of the anomalous tbW couplings. We find that in the limit of vanishing b quark mass, only the real part of coupling f_{2R} contributes to the spin density matrix at linear order. Because of the chiral structure of the anomalous tbW couplings, the resulting top polarizations are vastly different from those expected in the SM. We find that substantial deviations, as much as 20-30%, in the degree of longitudinal

top polarization from the SM value of -0.256 are possible even for anomalous couplings of magnitude 0.1 . The degree of longitudinal top polarization varies from -0.075 to -0.363 for Ref_{2R} while for Imf_{2R} it is symmetric around the SM value and varies from -0.139 to -0.139 with coupling varying from -0.2 to 0.2 as compared to the SM value of -0.256 for 14 TeV LHC.

Since top polarization can only be measured through the distributions of its decay products in top decay, we studied distributions of top decay products. We consider the top to decay semi-leptonically, since this channel is expected to have the best accuracy and spin analyzing power. However, decay distributions can get contributions from anomalous couplings responsible for top polarization as well as for top decay. We find that normalized charged-lepton azimuthal and energy distributions and b -quark azimuthal distributions are sensitive to anomalous couplings Ref_{2R} and Imf_{2R} . In each case, we define an asymmetry, whose deviation from the SM value would be a measure of the anomalous couplings. We find that the azimuthal asymmetry A_ϕ and the energy asymmetry A_{E_ℓ} of the charged lepton are more sensitive to negative values of the anomalous couplings Ref_{2R} . A limit of $[-0.034, 0.086]$ on Ref_{2R} would be possible from A_ϕ for cm energy of 14 TeV at the LHC with integrated luminosities of 10 fb^{-1} respectively. For Imf_{2R} the corresponding limit is ± 0.050 . A_{E_ℓ} , which is the most sensitive of the asymmetries we consider, probes Ref_{2R} and Imf_{2R} in the ranges $[-0.006, 0.009]$ and ± 0.038 respectively. Limits from A_b are the least stringent, though not much worse than those from A_{E_ℓ} .

The above results correspond to assuming only one coupling to be nonzero at a time. We also estimated simultaneous limits on Ref_{2R} and Imf_{2R} by combining measurements of all observables using a χ^2 analysis. The best possible 1σ limits on these couplings were found to be $[-0.010, 0.015]$ and $[-0.050, 0.050]$, respectively.

The limits we estimate for LHC with $\sqrt{s} = 7 \text{ TeV}$ and integrated luminosity 1 fb^{-1} are obviously worse. Nevertheless, they are comparable to those expected from an analysis of W helicities as carried out in [21].

In summary, our proposal will enable limits to be placed on f_{2R} which are somewhat better than limits expected from other measurements at the LHC, and at least an order of magnitude better than the indirect limits.

Our results would be somewhat worsened by the inclusion realistic detection efficiencies for the b jet and for the detection of the W . However, we would like to emphasize that since we do not require accurate reconstruction of the full top-quark four-momentum, the limits are not likely to be much worse. On the other hand, inclusion of the $\bar{t}W^+$ final state, as well as additional leptonic channels in top decay would contribute to improving on our estimates of the limits. A more complete analysis including detector simulation would be worthwhile to carry out.

Appendix

In this appendix, we give the spin density matrix elements for the single-top production process. For this we use the following notation for scalar products of four-momenta involved in the process: $(p_t \cdot p_b) = \mathcal{S}_{tb}$, $(p_t \cdot p_g) = \mathcal{S}_{tg}$ and $(p_b \cdot p_g) = \mathcal{S}_{bg}$. Also, we use the following

expressions :

$$\begin{aligned}
\mathcal{F}_1 = & \frac{g^2 g_s^2}{24 \mathcal{S}_{tg}^2 \mathcal{S}_{bg}^2} \left[\left\{ |f_{1L}|^2 \left(1 + \frac{m_t^2}{2m_W^2} \right) + 3 \text{Re} f_{1L} f_{2R}^* \frac{m_t}{m_W} + 3 |f_{2R}|^2 \frac{m_t^2}{2m_W^2} \right\} \right. \\
& \times \left\{ [\mathcal{S}_{tb} + \mathcal{S}_{tg} - \mathcal{S}_{bg}] [2\mathcal{S}_{tg} \mathcal{S}_{tb} \mathcal{S}_{bg} - m_t^2 \mathcal{S}_{bg}^2] - \mathcal{S}_{tg} \mathcal{S}_{bg} [\mathcal{S}_{bg}^2 - \mathcal{S}_{tg}^2] \right\} \\
& - |f_{1L}|^2 \frac{m_t^2}{m_W^2} \mathcal{S}_{tg}^2 \mathcal{S}_{bg}^2 + \text{Re} f_{1L} f_{2R}^* \frac{m_t}{m_W} \left\{ 2\mathcal{S}_{tg} \mathcal{S}_{bg}^2 [\mathcal{S}_{bg} - \mathcal{S}_{tg}] \right\} \\
& + \frac{|f_{2R}|^2}{m_W^2} \left\{ m_t^2 [-\mathcal{S}_{bg}^2 (\mathcal{S}_{bg} \mathcal{S}_{tg} - \mathcal{S}_{tb}^2 + \mathcal{S}_{bg}^2)] + \mathcal{S}_{tg} \mathcal{S}_{bg} [\mathcal{S}_{tb} (\mathcal{S}_{tg} + \mathcal{S}_{tb} - \mathcal{S}_{bg})] \right. \\
& \times \left. \left\{ 3(\mathcal{S}_{bg} - \mathcal{S}_{tg}) - \mathcal{S}_{tb} \right\} + \left\{ (\mathcal{S}_{bg} + \mathcal{S}_{tg})(\mathcal{S}_{bg}^2 - \mathcal{S}_{tg}^2) - \mathcal{S}_{tg}^3 \right\} \right\} \left. \right] \\
\mathcal{F}_2 = & \frac{g^2 g_s^2}{12 \mathcal{S}_{tg}^2 \mathcal{S}_{bg}^2} \left[\left\{ |f_{1L}|^2 \left(1 - \frac{m_t^2}{2m_W^2} \right) + \text{Re} f_{1L} f_{2R}^* \frac{m_t}{m_W} + |f_{2R}|^2 \frac{m_t^2}{2m_W^2} \right\} m_t \mathcal{S}_{bg} \right. \\
& \times [(\mathcal{S}_{bn} + \mathcal{S}_{gn}) \mathcal{S}_{tg} (\mathcal{S}_{tb} + \mathcal{S}_{tg}) - \mathcal{S}_{bg} (\mathcal{S}_{tb} \mathcal{S}_{gn} + \mathcal{S}_{tg} \mathcal{S}_{bn} + m_t^2 \mathcal{S}_{bn} - \mathcal{S}_{gn}) + \mathcal{S}_{tb} \mathcal{S}_{tg} \mathcal{S}_{bn}] \\
& - |f_{1L}|^2 \frac{m_t^2}{m_W^2} \mathcal{S}_{tg} \mathcal{S}_{bg}^2 \mathcal{S}_{gn} + \text{Re} f_{1L} f_{2R}^* \frac{1}{m_W} \left\{ 2\mathcal{S}_{tg}^2 \mathcal{S}_{bg} [\mathcal{S}_{tb} \mathcal{S}_{gn} - \mathcal{S}_{tg} \mathcal{S}_{bn}] \right\} \\
& + |f_{2R}|^2 \left\{ \mathcal{S}_{bn} (\mathcal{S}_{tb} - \mathcal{S}_{bg} + \mathcal{S}_{tg}) (m_t^2 \mathcal{S}_{bg}^2 - 3\mathcal{S}_{bg} \mathcal{S}_{tg}^2 + \mathcal{S}_{bg}^2 \mathcal{S}_{tg} - 2\mathcal{S}_{bg} \mathcal{S}_{tg} \mathcal{S}_{tb}) \right. \\
& + 2\mathcal{S}_{bg} \mathcal{S}_{tg}^2 \mathcal{S}_{tb} + \mathcal{S}_{gn} (\mathcal{S}_{tb} - \mathcal{S}_{bg} - \mathcal{S}_{tg}) (-\mathcal{S}_{bg} \mathcal{S}_{tg} \mathcal{S}_{tb} + \mathcal{S}_{bg} \mathcal{S}_{tg}^2 - \mathcal{S}_{bg}^3) - 2\mathcal{S}_{bg} \mathcal{S}_{tg}^3 \\
& \left. + \mathcal{S}_{bg}^2 (\mathcal{S}_{tb} \mathcal{S}_{bg} + 2\mathcal{S}_{bg} \mathcal{S}_{tg} + \mathcal{S}_{bg}^2 + m_t^2 \mathcal{S}_{tg}) \right\} \left. \right]
\end{aligned}$$

The diagonal elements of the spin density matrix for single-top production in tW channel can be written as

$$\rho(\pm, \pm) = \mathcal{F}_1 \pm \mathcal{F}_2 \quad (27)$$

with $\mathcal{S}_{gn} = (p_g \cdot n_3)$ and $\mathcal{S}_{bn} = (p_b \cdot n_3)$ and the off-diagonal elements are

$$\rho(\pm, \mp) = \mathcal{F}_2 \quad (28)$$

with $\mathcal{S}_{gn} = (p_g \cdot (n_1 \pm i n_2))$ and $\mathcal{S}_{bn} = (p_b \cdot (n_1 \pm i n_2))$ where n_i^μ 's ($i = 1, 2, 3$) are the four-vectors with the properties $n_i \cdot n_j = -\delta_{ij}$ and $n_i \cdot p_t = 0$. n_1, n_2 and n_3 represent spin four-vectors of the top quark with spin respectively along the x, y and z axis in the top rest frame.

-
- [1] F. Abe *et al.* [CDF Collaboration], Phys. Rev. Lett. **73**, 225 (1994) [arXiv:hep-ex/9405005].
 - [2] [CDF and D0 Collaboration], arXiv:hep-ex/0703034.
 - [3] I. I. Y. Bigi, Y. L. Dokshitzer, V. A. Khoze, J. H. Kuhn and P. M. Zerwas, Phys. Lett. B **181**, 157 (1986).
 - [4] K. Huitu, S. K. Rai, K. Rao, S. D. Rindani, P. Sharma, JHEP **1104**, 026 (2011) [arXiv:1012.0527 [hep-ph]].

- [5] M. Arai, K. Huitu, S. K. Rai, K. Rao, JHEP **1008**, 082 (2010) [arXiv:1003.4708 [hep-ph]].
- [6] R. M. Godbole, K. Rao, S. D. Rindani, R. K. Singh, JHEP **1011**, 144 (2010) [arXiv:1010.1458 [hep-ph]].
- [7] D. Choudhury, R. M. Godbole, S. D. Rindani, P. Saha, [arXiv:1012.4750 [hep-ph]].
- [8] E. L. Berger, Q. -H. Cao, C. -R. Chen, H. Zhang, [arXiv:1103.3274 [hep-ph]].
- [9] A. Heinson, A. S. Belyaev, E. E. Boos, Phys. Rev. **D56**, 3114-3128 (1997) [hep-ph/9612424].
- [10] T. Stelzer, Z. Sullivan and S. Willenbrock, Phys. Rev. D **58**, 094021 (1998) [arXiv:hep-ph/9807340].
- [11] A. S. Belyaev, E. E. Boos and L. V. Dudko, Phys. Rev. D **59**, 075001 (1999) [arXiv:hep-ph/9806332].
- [12] E. Boos, L. Dudko and T. Ohl, Eur. Phys. J. C **11**, 473 (1999) [arXiv:hep-ph/9903215].
- [13] T. M. P. Tait, Phys. Rev. D **61**, 034001 (2000) [arXiv:hep-ph/9909352].
- [14] D. Espriu and J. Manzano, Phys. Rev. D **65**, 073005 (2002) [arXiv:hep-ph/0107112].
- [15] D. Espriu and J. Manzano, Phys. Rev. D **66**, 114009 (2002) [arXiv:hep-ph/0209030].
- [16] T. M. P. Tait and C. P. P. Yuan, Phys. Rev. D **63**, 014018 (2000) [arXiv:hep-ph/0007298].
- [17] T. Aaltonen *et al.* [The CDF Collaboration], Phys. Rev. Lett. **105**, 042002 (2010) [arXiv:1003.0224 [hep-ex]].
- [18] V. M. Abazov *et al.* [D0 Collaboration], Phys. Rev. D **83**, 032009 (2011) [arXiv:1011.6549 [hep-ex]].
- [19] C. R. Chen, F. Larios and C. P. Yuan, Phys. Lett. B **631**, 126 (2005) [AIP Conf. Proc. **792**, 591 (2005)] [arXiv:hep-ph/0503040].
- [20] G. Aad *et al.* [ATLAS Collaboration], Report No. ATLAS-CONF-2011-037; S. Chatrchyan *et al.* [CMS Collaboration], arXiv:1104.3829 [hep-ex].
- [21] J. A. Aguilar-Saavedra, N. F. Castro and A. Onofre, Phys. Rev. D **83**, 117301 (2011) [arXiv:1105.0117 [hep-ph]].
- [22] S. Chatrchyan *et al.* [CMS Collaboration], arXiv:1106.3052 [hep-ex].
- [23] J. A. Aguilar-Saavedra, J. Carvalho, N. F. Castro, F. Veloso and A. Onofre, Eur. Phys. J. C **50**, 519 (2007) [arXiv:hep-ph/0605190].
- [24] W. Bernreuther, P. Gonzalez, M. Wiebusch, Eur. Phys. J. **C60**, 197-211 (2009) [arXiv:0812.1643 [hep-ph]].
- [25] P. L. Cho and M. Misiak, Phys. Rev. D **49**, 5894 (1994) [arXiv:hep-ph/9310332].
- [26] F. Larios, M. A. Perez and C. P. Yuan, Phys. Lett. B **457**, 334 (1999) [arXiv:hep-ph/9903394].
- [27] G. Burdman, M. C. Gonzalez-Garcia and S. F. Novaes, Phys. Rev. D **61**, 114016 (2000) [arXiv:hep-ph/9906329].
- [28] B. Grzadkowski, M. Misiak, Phys. Rev. **D78**, 077501 (2008) [arXiv:0802.1413 [hep-ph]].
- [29] B. Grzadkowski and Z. Hioki, Phys. Lett. **B476**, 87 (2000) [arXiv:hep-ph/9911505]; S. D. Rindani, Pramana **54**, 791 (2000) [arXiv:hep-ph/0002006]; B. Grzadkowski and Z. Hioki, Phys. Lett. **B529**, 82 (2002) [arXiv:hep-ph/0112361]; Phys. Lett. **B557**, 55 (2003) [arXiv:hep-ph/0208079]; Z. Hioki, arXiv:hep-ph/0104105 and arXiv:hep-ph/0210224; K. Ohkuma, Nucl. Phys. Proc. Suppl. **111**, 285 (2002) [arXiv:hep-ph/0202126].
- [30] R. M. Godbole, S. D. Rindani and R. K. Singh, JHEP **0612**, 021 (2006) [arXiv:hep-ph/0605100].
- [31] M. Beccaria, F. M. Renard and C. Verzegnassi, Phys. Rev. D **71**, 033005 (2005) [arXiv:hep-ph/0410089].
- [32] J. A. M. Vermaseren, arXiv:math-ph/0010025.
- [33] J. Pumplin, A. Belyaev, J. Huston, D. Stump and W. K. Tung, JHEP **0602**, 032 (2006)

- [arXiv:hep-ph/0512167].
- [34] W. Bernreuther, J. Phys. G **G35**, 083001 (2008) [arXiv:0805.1333 [hep-ph]].
 - [35] F. Hubaut, E. Monnier, P. Pralavorio, K. Smolek and V. Simak, Eur. Phys. J. C **44S2**, 13 (2005) [arXiv:hep-ex/0508061].
 - [36] J. A. Aguilar-Saavedra, J. Carvalho, N. F. Castro, A. Onofre, F. Veloso, Eur. Phys. J. **C53**, 689-699 (2008) [arXiv:0705.3041 [hep-ph]].
 - [37] J. A. Aguilar-Saavedra, Nucl. Phys. **B804**, 160-192 (2008) [arXiv:0803.3810 [hep-ph]].
 - [38] J. A. Aguilar-Saavedra, J. Bernabeu, Nucl. Phys. **B840**, 349-378 (2010) [arXiv:1005.5382 [hep-ph]].
 - [39] M. M. Najafabadi, JHEP **0803**, 024 (2008) [arXiv:0801.1939 [hep-ph]].
 - [40] A. Lucotte, A. Llres, D. Chevallier, ATLAS note ATL-PHYS-PUB-2007-005.
 - [41] S. Zhu, arXiv:hep-ph/0109269.
 - [42] M. Beccaria, C. M. Carloni Calame, G. Macorini, G. Montagna, F. Piccinini, F. M. Renard, C. Verzegnassi, Eur. Phys. J. **C53**, 257-265 (2008) [arXiv:0705.3101 [hep-ph]].
 - [43] The expressions for charged-lepton and b -quark angular distributions agree with those given in Ref. [38]
 - [44] [a, b] denotes the allowed values of the coupling f at the 1σ level, satisfying $a < f < b$.